ChemistrySelect

Research Article
doi.org/10.1002/slct.202301641

Chemistry Europe
European Chemical Societies Publishing

www.chemistryselect.org

Imidazole-hydrazone derivatives: Synthesis, characterization, X-ray structures and evaluation of anticancer and carbonic anhydrase I–II inhibition properties

Hakan Ünver,[a] Ulviye Acar Cevik,*[b] Hayrani Eren Bostancı,[c] Oğuzhan Kaya,[c] and Ümit M. Kocyigit[c]

The nine new imidazole-hydrazone derivatives of Schiff base were synthesized from the condensation reactions of 1-methyl-1*H*-imidazole-2-carbaldehyde with various substituted-hydrazide derivatives. Structures of the final compounds (**1a**–**1i**) were characterized by using ^{1}H NMR, ^{13}C NMR spectroscopic techniques, elemental analysis, and crystal X-ray diffraction. The *in vitro* carbonic anhydrase I and II potentials of these synthesized were evaluated. The result suggests that compound **1a**, a 4-methoxy substituted analog with an IC_{50} of 0.949 μM, was found to have the most potent hCA I inhibitory activity. Compounds **1c**, **1d**, and **1h** were the most potent compounds on hCA II with IC_{50} values of 3.330, 4.454, and 5.66 μM, respectively. All compounds were examined for their cytotoxicity towards human colorectal adenocarcinoma cell (HT29) and rat glioma cell line (C6) compared to mouse fibroblast normal cell line (L929) using the MTT assay method. The compounds **1a**, **1d**, and **1i** exhibited significant antiproliferative activity with less toxicity to a health cell line. Consequently, compound **1a** could be the potential lead for emerging selective cytotoxic compounds directing hCA I. Compound **1d** could be the potential lead for emerging selective cytotoxic compounds directing hCA II.

Introduction

Cancer is the second leading cause of death worldwide after cardiac disease, is characterized as the uncontrolled growth of abnormal cells anywhere in the body. Many drugs have been discovered for the treatment of cancer. However, side effects, drug resistance, severe toxicity, and low selectivity are the major disadvantages of current drugs. Therefore, it is vital to create new anticancer medications that are very effective and targeted.[1]

Carbonic anhydrases (CAs), which are enzymes that catalyze the interconversion of CO_2 and HCO^{3-}, are present in several organisms.[2] There are now 15 distinct isoforms known, each with a unique molecular structure, catalytic capabilities, organ and tissue distribution, subcellular localization, and capacity to interact with various inhibitor types.[3] There are various cytosolic forms (CA I, II, III, and IV) seen in mammals. Four of these forms are membrane-bound (CA IV, IX, XII, and XIV), secreted (CA VI), and mitochondrial (CA VA, VB).[4] Fluctuations in CA expression levels can cause cancer, neuropathic pain, altitude sickness, glaucoma, epilepsy, hypertension, and more. In light of this, numerous hCA isoforms are regarded as desirable therapeutic targets for various pharmacological uses.[5,6] The precise physiological significance of CA I, which is widely distributed across many tissues and contributes to various pathological conditions such as retinal and brain edema, is poorly unknown. Additionally, abundant in numerous tissues, CA II is important in many disease states, including glaucoma, epilepsy, edema, high altitude condition, and kidney illness.[7] Furthermore, several tumor cells and cell lines have been found to exhibit CAI and CAII.[8]

The heterocycles that include nitrogen are among a group of substances with a wealth of practical uses. Small-molecule pharmaceuticals of fused nitrogen heterocycles make up 59% of U.S. FDA-approved medicines, particularly in the pharmaceutical industry. Among the top twenty-five nitrogen-containing heterocycles found in small molecule medications, imidazole is one of the heterocycles that contain nitrogen. This ring is an essential building block developing new drug candidates because it is an essential part of structural scaffolds seen in contemporary medicinal chemistry.[9] The bioactivity of molecules with an imidazole ring has been found to include anticancer,[10] antioxidant,[11] antibacterial,[12] antiviral,[13] antitubercular[14] and antifungal[15] properties.

Additionally, due to their significant biological and pharmacological characteristics, hydrazides-hydrazones bearing the azomethine (ArCONHN=CH) moiety have become a crucial foundation for the synthesizing active medicines. The activity of hydrazide-hydrazone fragments bound to heterocyclic systems is enhanced by their capacity to form hydrogen bonds with the molecular target.[16] This discovery has had a substantial impact

[a] *Assoc. Prof. H. Ünver*
Department of Chemistry, Faculty of Science,
Eskisehir Technical University, Eskisehir, Turkey

[b] *Assoc. Prof. U. Acar Cevik*
Department of Pharmaceutical Chemistry,
Faculty of Pharmacy, Anadolu University,
Eskişehir 26470, Turkey
E-mail: uacar@anadolu.edu.tr

[c] *Dr. H. E. Bostancı, O. Kaya, Assoc. Prof. Ü. M. Kocyigit*
Department of Biochemistry, Faculty of Pharmacy,
Cumhuriyet University, Sivas, Turkey

Supporting information for this article is available on the WWW under https://doi.org/10.1002/slct.202301641

on medical chemistry. These compounds' acetylcholinesterases,[17] anticancer,[18] α-glucosidase,[19] antitubercular,[20] anti-mitotic,[21] antimicrobial,[22] and antifungal[23] properties are also of great interest.

In this study, it was aimed to synthesize new imidazole-hydrazone derivatives and test their carbonic anhydrase inhibitory effects on hCA I and II isoenzymes. It was also planned to investigate their cytotoxic activities towards two cancer cell lines (C6 and HT-29) and one non-tumor cell line (L929). The structure of compounds was elucidated using various spectral techniques, including ^{1}H NMR, ^{13}C NMR, elemental analysis, and crystal X-ray diffraction.

Results and Discussion

Chemistry

The general structures of hydrazones **1 a**–**1 i** synthesized in this study are shown in Figure 1. A mixture of different hydrazide derivatives and 1-methyl-1*H*-imidazole-2-carbaldehyde was dissolved in ethanol. The mixture was refluxed for 4–6 h to obtain hydrazone derivatives. The proposed mechanism for the reaction of 1-methyl-1*H*-imidazole-2-carbaldehyde with hydrazine hydrate is given in Figure 2. The structure of title compounds was determined using data obtained from ^{1}H NMR, ^{13}C NMR, elemental analysis, and crystal X-ray diffraction.

The ^{1}H NMR spectra of the compound, the hydrogens of the methyl group of compounds were observed at the range of 3.40–4.27 ppm. The singlet signals at 11.39–15.05 ppm and 7.72–8.42 ppm in all of the spectra (O=C-NH) and N=CH, respectively, verified the *N*-acylhydrazone skeleton in the structures of compounds **1 a**–**1 i**. In the ^{1}H NMR spectra, a single signal at 3.89–3.97 ppm was generated by the protons of the methoxy substituent (compounds **1 a** and **1 i**). Aromatic protons attached to imidazole and phenyl ring were observed in the range of 7.05–8.38 ppm.

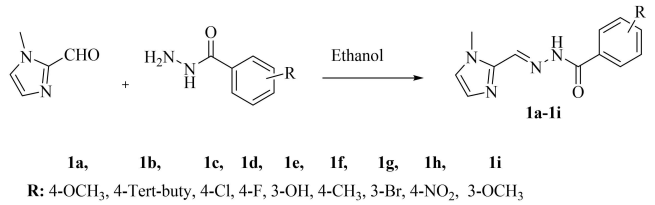

Figure 1. General procedure for synthesis of the final compounds **1 a**–**1 i**.

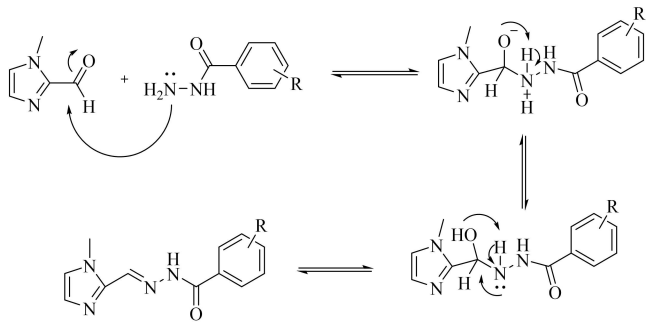

Figure 2. Reaction mechanism of compounds **1 a**–**1 i.**

^{13}C NMR spectra of these compounds, –CH_3 and –OCH_3 carbons showed signals around 33.0 ppm and 55.0 ppm, respectively. The CH=N signal appeared near 140.0 ppm in the aromatic region. Compounds (**1 a**–**1 i**) displayed characteristic (C=O) signals at 155.68–163.56 ppm.

Structural Analysis

Both compounds X-ray suitable crystals were obtained by layer diffusion of diethyl ether into methanolic solutions. MERCURY structures of compounds are given in Figure 3. Crystal parameters, bond distances and angles are given in Tables 1 and 2.

Compound **1 a** crystallized in $P2_1/c$ space group of the monoclinic system. Compound unit cell composed of one complete molecule. Unit cell dimensions are $a = 17.371(3)$ Å, $\alpha = 90°$, $b = 4.0607(6)$ Å, $\beta = 114.513(5)°$, $c = 19.414(3)$ Å, $\gamma = 90°$ and $V = 1246.0(3)$ Å^3. The C–N bond lengths range from 1.290(3) to 1.463(3) Å and the C–O bond lengths range from 1.217(3) to

Table 1. Crystal data and structure refinement for compounds **1 a** and **1 f.**

Compound	**1 a**	**1 f**
CCDC number	: 2246383	: 2246382
Empirical formula	: $C_{13}H_{14}N_4O_2$	: $C_{13}H_{14}N_4O$
Formula weight	: 258.28	: 242.28
Temperature/K	: 273.15	: 273.15
Crystal system	: Monoclinic	: Monoclinic
Space group	: $P2_1/c$	: $P2_1/n$
a/Å	: 17.371(3)	: 15.1168(18)
α/°	: 90	: 90
b/Å	: 4.0607(6)	: 4.8748(5)
β/°	: 114.513(5)	: 105.230(4)
c/Å	: 19.414(3)	: 17.094(2)
γ/°	: 90	: 90
Volume/Å^3	: 1246.0(3)	: 1215.5(2)
Z	: 4	: 4
ϱcalcg/cm^3	: 1.377	: 1.324
μ/mm^{-1}	: 0.097	: 0.089
F(000)	: 544.0	: 512.0
Crystal size/mm^3	: 0.09×0.08×0.05	: 0.16×0.13×0.11
2Θ range for data collection/°	: 4.612 to 54.276	: 4.94 to 53.432
Index ranges	$-22 \le h \le 22$, $-5 \le k \le 5$, $-24 \le l \le 24$	$-19 \le h \le 19$ $-6 \le k \le 6$ $-21 \le l \le 21$
Reflections collected	: 23264	: 31905
Completeness to theta	: 27.138, 99.7%	: 26.716, 99.7%
Absorption correction	: Multi-Scan	: Multi-Scan
Refinement method	: Full-matrix least-squares on F^2	: Full-matrix least-squares on F^2
Independent reflections	: 2753, [Rint = 0.0969 Rsigma = 0.0774]	: 2569, [Rint = 0.0882 Rsigma = 0.0586]
Data/restraints/parameters	: 2753/0/175	: 2569/0/166
Goodness-of-fit on F^2	: 1.023	: 1.025
Final R indexes [I > = 2σ (I)]	: R1 = 0.0522, wR2 = 0.0979	: R1 = 0.0492, wR2 = 0.1100
Final R indexes [all data]	: R1 = 0.1389, wR2 = 0.1314	: R1 = 0.1145, wR2 = 0.1372
Largest diff. peak/hole/e Å^{-3}	: 0.20/−0.17	: 0.18/−0.17

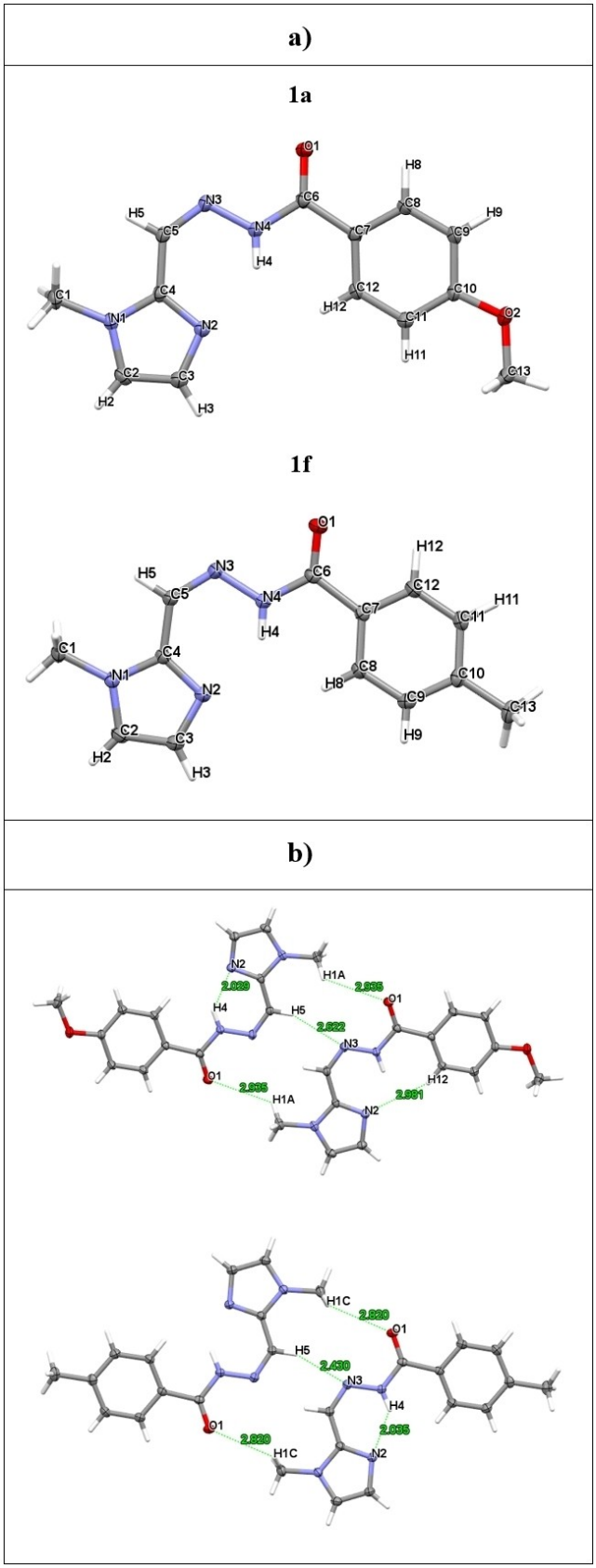

Figure 3. a) Thermal ellipsoid plots of compounds **1 a** and **1 f** at the 20 % probability level. **b)** *inter-* and *intra-* Hydrogen bonding interactions.

Table 2. Selected bond distances (Å) and angles (°) for compounds **1 a** and **1 f**.

Compound **1 a**	
Bond Distances (Å)	Bond Angles (°)
C(1)–N(1) 1.463(3)	C(1)–N(1)–C(4) 127.9(2)
C(4)–N(1) 1.366(3)	N(1)–C(4)–C(5) 122.5(2)
C(4)–N(2) 1.331(3)	C(4)–C(5)–N(3) 129.3(2)
C(5)–N(3) 1.290(3)	N(3)–N(4)–C(6) 120.38(19)
N(3)–N(4) 1.367(2)	N(4)–C(6)–O(1) 122.5(2)
N(4)–C(6) 1.365(3)	C(6)–C(7)–C(8) 117.7(2)
C(6)–O(1) 1.217(3)	C(10)–O(2)–C(13) 117.8(2)
O(2)–C(10) 1.368(3)	
O(2)–C(13) 1.421(3)	
Compound **1 f**	
Bond Distances (Å)	Bond Angles (°)
C(1)–N(1) 1.458(3)	C(1)–N(1)–C(4) 127.11(17)
C(4)–N(1) 1.363(2)	N(1)–C(4)–C(5) 122.22(18)
C(4)–N(2) 1.338(2)	C(4)–C(5)–N(3) 128.90(19)
C(5)–N(3) 1.287(2)	N(3)–N(4)–C(6) 120.15(16)
N(3)–N(4) 1.368(2)	N(4)–C(6)–O(1) 123.03(19)
N(4)–C(6) 1.364(2)	C(6)–C(7)–C(8) 124.67(18)
C(6)–O(1) 1.225(2)	C(10)–C(13)–C(9) 121.7(2)
C(13)–C(10) 1.505(3)	

1.421(3) Å. It was observed that, the crystal was stacked in the Z isomer structure. The selected bond angles range between 117.7(2)° and 129.3(2)°.

Compound **1 f** crystallized in $P2_1/n$ space group of the monoclinic system. Unit cell composed of one complete molecule. Unit cell dimensions are $a = 15.1168(18)$ Å, $\alpha = 90°$, $b = 4.8748(5)$ Å, $\beta = 105.230(4)°$, $c = 17.094(2)$ Å, $\gamma = 90°$ and $V = 1215.5(2)$ Å^3. The C–N bond lengths range from 1.287(2) to 1.458(3) Å and a C–O bond length of 1.225(2) Å. The crystal was stacked in the Z isomer structure as also compound **1 a**. The selected bond angles range between 120.15(16)° and 128.90(19)°. In the crystal packing structures of both compounds, there are some intra- and inter-molecular hydrogen bonding interactions are also observed.

Anticancer Activity

HT29, C6, and L929 cell lines were used to test the cytotoxic effects of compounds **1 a**–**1 i**. The concentration of the derivative that causes the 50 % inhibition of cell survivability (IC_{50}) was calculated (Table 3). Cisplatin was used as the reference drug in the MTT test.

Table 3. IC_{50} values (μM) of the compounds **1 a**–**1 i** and cisplatin against C6, HT29 and L929.

Comp.	C6	HT29	L929
1a	75,59 ± 9,56	68,96 ± 11,52	> 100
1b	17,78 ± 0,26	20,37 ± 2,59	7,67 ± 0,67
1c	> 100	> 100	89,53 ± 1,43
1d	> 100	70,10 ± 8,79	> 100
1e	> 100	> 100	> 100
1f	> 100	95,36 ± 18,69	> 100
1 g	> 100	> 100	80,75 ± 5,85
1 h	> 100	> 100	90,28 ± 4,55
1i	86,79 ± 13,36	69,93 ± 1,58	> 100
Cis-platin	157,35 ± 18,06	127 ± 15,34	173,64 ± 4,42

Compared to the reference drug cisplatin, there is a higher efficacy of compounds **1a**, **1b**, **1d**, **1f**, and **1i** against HT29 cell line. Among these compounds, compound **1b** has the highest activity. However, when the effect of compound **1b** on the healthy cell line (L929) is examined, it is seen that this compound is cytotoxic. The cytotoxic effect of compounds **1a**, **1d**, **1f** and **1i** against the HT-29 cell line is higher than that of the L929 cell line. This shows that the selectivity of these compounds against healthy cells is high.

Compounds **1a**, **1b**, and **1i** were assayed for their abilities to inhibit the C6 cell line compared to cisplatin. Among these compounds, compound **1b** has the highest activity against the C6 cell line. Considering its selectivity on the healthy cell line, compound **1a** was chosen as the best compound against the C6 cell line.

Carbonic Anhyrase I/II Inhibition Assay

Research on carbonic anhydrases (CAs) has holistically revealed their important role in diseases such as glaucoma, obesity, osteoporosis, cancer, high altitude sickness, epilepsy, neuropathic pain, and sleep apnea. hCA I is widely found in various tissues and is known to be involved in some pathological conditions, such as retinal and brain edema, although its physiological function is largely a mystery.[24] hCA II is abundant in many tissues and plays an important role in the emergence of many diseases such as glaucoma, epilepsy, edema, high altitude sickness, and kidney disorders.[25] The discovery of new carbonic anhydrase inhibitors is significant due to the many side effects of carbonic anhydrase inhibitors used in treating these diseases today. For this purpose, the effects of these newly synthesized imidazole-hydrazone derivatives (**1a**–**1i**) on these enzymes were investigated and the obtained values are given in Table 4 and Figure 4. The IC_{50} graphs of compounds **1a** and **1c** are given in Figure 5.

The synthesized imidazole-hydrazone derivatives (**1a**–**1i**) exhibited general inhibition profiles against widespread cytosolic hCA I isozyme with IC_{50} values ranging from 0.949 μM to 14.461 μM and cytosolic hCA II isozyme with IC_{50} values ranging from 3.330 μM to 30.4192 μM. However, the inhibition potentials of these molecules are less than the standard substance AAZ.

The most active compound **1a** showed IC_{50} values of 0.949 μM on hCA I. The other derivative that showed notable inhibitory effects on hCA I isoform was compound **1g** with IC_{50} value 1.207 μM.

For hCA I, IC_{50} values of acetazolamide (AAZ) as positive control and the novel compounds were studied in this study the following order: AAZ (0.772 μM, r^2: 0.961) < **1a** (0.949 μM, r^2: 0.865) < **1g** (1.207 μM, r^2: 0.802) < **1e** (3.292 μM, r^2: 0.925) < **1c** (3.559 μM, r^2: 0.906) < **1d** (3.659 μM, r^2: 0.981) < **1h** (5.142 μM,

Table 4. The summarized inhibition parameters of synthesized imidazole-hyrazone derivatives (**1a**–**1i**) towards human carbonic anhydrase I and II isoforms.

Compound	IC_{50} (μM) hCA I	r^2	hCA II	r^2
1a	0.949	0.865	14.689	0.905
1b	8.990	0.915	14.607	0.938
1c	3.559	0.906	3.330	0.959
1d	3.659	0.981	4.454	0.953
1e	3.292	0.925	6.523	0.951
1f	14.461	0.984	18.476	0.920
1 g	1.207	0.802	7.947	0.936
1 h	5.142	0.993	5.669	0.813
1i	13.359	0.934	30.192	0.882
AAZ	0.772	0.961	6.383	0.933

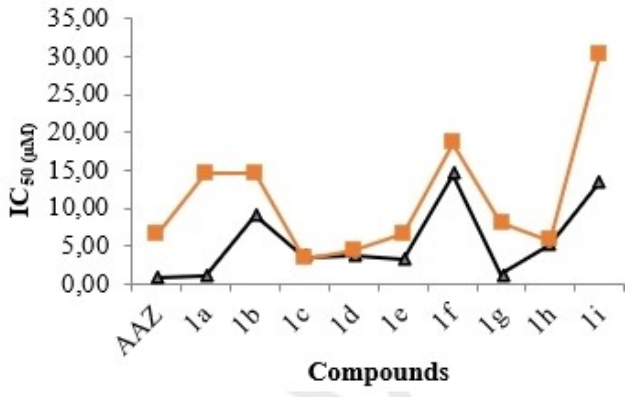

Figure 4. The summarized inhibition parameters of synthesized hydrazones derivatives (**1a-1i**) towards human carbonic anhydrase I and II isoforms.

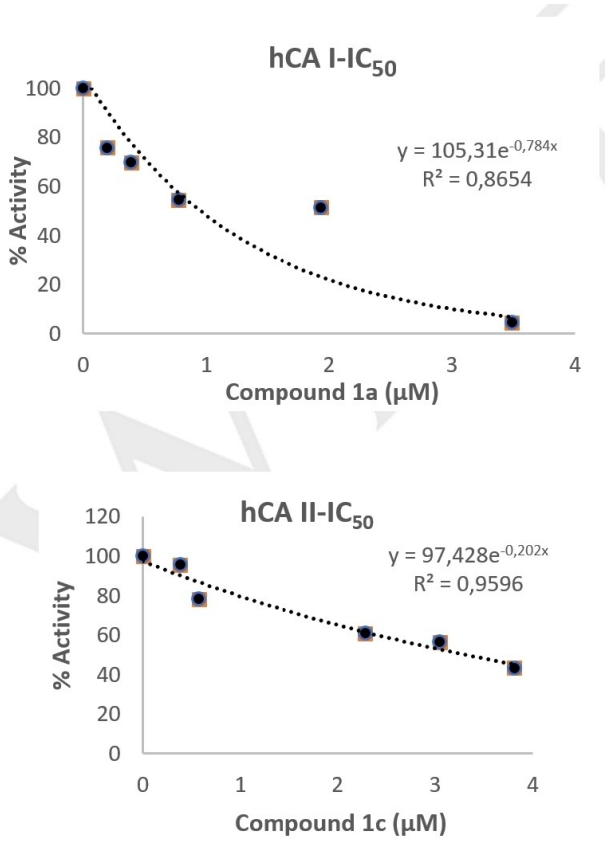

Figure 5. IC_{50} graphs of molecules showing the best inhibitor potential

r^2: 0.993) < **1 b** (8.990 μM, r^2: 0.915) < **1 i** (13.359 μM, r^2: 0.934) < **1 f** (14.461 μM, r^2: 0.984).

The most active compound **1 c** showed IC_{50} values of 3.330 μM on hCA II. The other derivatives that showed notable inhibitory effects on hCA I isoform were compounds **1 d** and **1 h** with IC_{50} values ranging between 4.454 and 5.669 μM. For hCA II, IC_{50} values of acetazolamide (AAZ) as positive control and the novel compounds were studied in this study the following order: **1 c** (3.330 μM, r^2: 0.959) < **1 d** (4.454 μM, r^2: 0.953) < **1 h** (5.669 μM, r^2: 0.813) < **AAZ** (6.383 μM, r^2: 0.933) < **1 e** (6.523 μM, r^2: 0.951) < **1 g** (7.947 μM, r^2: 0.936) < **1 b** (14.607 μM, r^2: 0.938) < **1 a** (14.689 μM, r^2: 0.905) < **1 f** (18.476 μM, r^2: 0.920) < **1 i** (30.192 μM, r^2: 0.882). According to these data, it has been observed that these molecules have the potential to inhibit these enzymes.

Structural activity relationship [SAR] studies

The structural activity relationship investigations of new imidazole-hydrazone derivatives (**1 a-1 i**) were performed for their cytotoxic activity using C6, HT29, and L929 cancer cell lines. The SAR study of the compounds is given in Figure 6.

In the synthesized derivatives, compound **1 a** demonstrates the highest carbonic anhydrase I inhibitor activity compared to other compounds, mainly attributed to electron releasing methoxy groups at the *para* position of the phenyl ring. It is observed that carbonic anhydrase I inhibitory activity decreases with the *meta*-position of the methoxy group. It is observed that carbonic anhydrase II inhibitor activity increases with electron-withdrawing groups (Cl, F, NO_2) in the para position of the phenyl ring (compounds **1 c**, **1 d**, and **1 h**).

It was determined that compound **1 a**, which has high carbonic anhydrase I activity, has a high activity on cancer cells. With the 3rd position of the methoxy group (compound **1 i**), it is seen that the cancer activity continues, but the activity on the carbonic anhydrase I enzyme decreases. In addition, it is seen that both compound **1 a** and compound **1 i** have high selectivity in healthy cells.

Conclusions

The newly designed compounds **1 a**–**1 i**, 3/4-Substituted-*N*′-((1-methyl-1*H*-imidazol-2-yl)methylene) benzohydrazide, were synthesized, and their structure was characterized with spectroscopic methods. Their potential cytotoxic activities and inhibitory activities towards hCA I and hCA II enzymes were evaluated. The synthesized imidazole-hydrazone derivatives (**1 a**–**1 i**) exhibited general inhibition profiles against widespread cytosolic hCA I isozyme with IC_{50} values ranging from 0.949 μM to 14.461 μM and cytosolic hCA II isozyme with IC_{50} values ranging from 3.330 μM to 30.4192 μM. However, the inhibition potentials of these molecules are less than the standard drug AAZ. The most active compounds were **1 a** with IC_{50} = 0.949 μM against hCA I, whereas compound **1 c** showed good inhibition against hCA II with IC_{50} = 3.330 μM. All compounds were examined for their cytotoxicity towards human colorectal adenocarcinoma cell (HT29) and rat glioma cancer cell line (C6) compared to mouse fibroblast normal cell line (L929) using the MTT assay method. Compound **1 b** was found to be the most potent derivative against C6 (IC_{50}: 17,78 ± 0,26 μM) and HT29 (IC_{50} = 20,37 ± 2,59 μM). However, compound **1 b** appears toxic in a healthy cell line (L929). Considering the selectivity of the compounds on the healthy cell (L929), compound **1 a** was found to be the most potent derivative against C6 (IC_{50} = 75,59 ± 9,56 μM), HT29 (IC_{50} = 5.87 ± 0.37 μM).

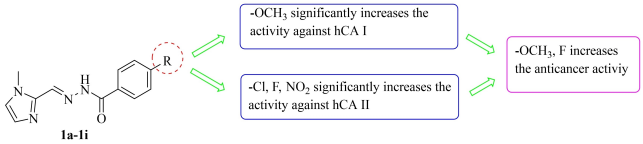

Figure 6. SAR study of the synthesized compounds **1a**–**1i**

Experimental Section

Chemistry

All the chemicals employed in the synthetic procedure were purchased from Sigma-Aldrich Chemicals (Sigma-Aldrich Corp., St. Louis, MO, USA) or Merck Chemicals (Merck KGaA, Darmstadt, Germany). Melting points of the obtained compounds were determined by MP90 digital melting point apparatus (Mettler Toledo, OH, USA) and were uncorrected. ^{1}H-NMR, and ^{13}C-NMR spectra of the synthesized compounds were performed by a Bruker 400 MHz and 100 MHz digital FT-NMR spectrometer (Bruker Bioscience, Billerica, MA, USA) in DMSO-d_6, respectively. Splitting patterns were designated as follows: s: singlet; d: doublet; t: triplet; m: multiplet in the NMR spectra. Coupling constants (*J*) were reported as Hertz. All reactions were monitored by thin-layer chromatography (TLC) using Silica Gel 60 F254 TLC plates (Merck KGaA, Darmstadt, Germany).

Deposition numbers CCDC 2246383 (for **1 a**), 2246382 (for **1 f**) contain(s) the supplementary crystallographic data for this paper. These data are provided free of charge by the joint Cambridge Crystallographic Data Centre and Fachinformationszentrum Karlsruhe Access Structures service.

Synthesis of 4-substitue/3-substitue*-N′-*((1-methyl-1*H*-imidazol-2-yl)methylene)benzohydrazide derivatives (1 a–1 i):

The hydrazide derivatives (0.003 mol) and 1-methyl-1*H*-imidazole-2-carbaldehyde (0.003 mol) were dissolved in ethanol and refluxed for 4 hours. After the end of the reaction was controlled by TLC control, the precipitated product was filtered.

4-Methoxy-*N*′-((1-methyl-1*H*-imidazol-2-yl)methylene) benzohydrazide (1 a): Yield: 76%. M.P. 188–190 °C. ^{1}H-NMR (400 MHz, DMSO-d_6): δ = 3.84 (3H, s, CH_3), 3.89 (3H, s, OCH_3), 7.11 (2H, d, *J* = 8.48 Hz, 1,4-disubstituebenzen), 7.33 (1H, s, imidazole CH), 7.43 (1H, s, imidazole CH), 7.72 (1H, s, CH=N), 7.90 (2H, d, *J* = 8.52 Hz, 1,4-disubstituebenzen), 14.64 (1H, s, NH). ^{13}C-NMR (100 MHz, DMSO-d_6): δ = 33.60 (CH_3), 55.99 (OCH_3), 114.83, 124.04, 125.55, 128.06, 128.63, 129.15, 129.61, 141.47, 162.84 (C=O). Anal. calcd. For $C_{13}H_{14}N_4O_2$, C, 60.45; H, 5.46; N, 21.69. Found: C, 60.53; H, 5.47; N, 21.71.

4-Tert-butyl-*N*′-((1-methyl-1*H*-imidazol-2-yl)methylene) benzohydrazide (1 b): Yield: 73 %. M.P. 202–204 °C. ^{1}H-NMR (400 MHz, DMSO-d_6): δ = 1.50 (9H, s, CH_3), 4.08 (3H, s, CH_3), 7.61–7.53 (2H, m, 1,4-disubstituebenzen), 7.78–7.80 (2H, m, imidazole CH), 7.93 (1H, s, CH=N), 8.05-8.07 (2H, m, 1,4-disubstituebenzen). ^{13}C-NMR (100 MHz, DMSO-d_6): δ = 31.29, 33.52, 35.20, 124.01, 125.76, 126.33, 127.50, 127.90, 128.61, 129.46, 130.63, 155.68. Anal. calcd. For $C_{16}H_{20}N_4O$, C, 67.58; H, 7.09; N, 19.70. Found: C, 67.71; H, 7.10; N, 19.73.

4-Chloro-*N*′-((1-methyl-1*H*-imidazol-2-yl)methylene) benzohydrazide (1 c): Yield: 68 %. M.P. 227–230 °C. ^{1}H-NMR (400 MHz, DMSO-d_6): δ = 3.40 (3H, s, CH_3), 6.62 (1H, s, Aromatic CH), 6.73–6.75 (1H, m, Aromatic CH), 6.92 (1H, s, imidazole CH), 7.01–7.06 (3H, d, *J* = 8.40 Hz, 1,4-disubstituebenzen, imidazole CH), 7.99 (1H, s, CH=N), 11.39 (1H, s, NH). ^{13}C-NMR (100 MHz, DMSO-d_6): δ = 35.54 (CH_3), 124.21, 126.18, 128.73, 129.17, 129.66, 130.05, 137.18, 140.99, 162.45 (C=O). Anal. calcd. For $C_{12}H_{11}ClN_4O$, C, 54.87; H, 4.22; N, 21.33. Found: C, 55.02; H, 4.21; N, 21.40.

4-Fluoro-*N*′-((1-methyl-1*H*-imidazol-2-yl)methylene) benzohydrazide (1 d): Yield: 71 %. M.P. 180–185 °C. ^{1}H-NMR (400 MHz, DMSO-d_6): δ = 3.90 (3H, s, CH_3), 7.34 (1H, br.s., Aromatic CH), 7.44 (3H, br.s. Aromatic CH), 7.77 (1H, s, CH=N), 7.99 (2H, br.s. 1,4-disubstituebenzen). ^{13}C-NMR (100 MHz, DMSO-d_6): δ = 33.63 (CH_3), 116.56, 116.78, 124.17, 128.71, 128.84, 130.08, 130.37, 141.40, 162.35 (C=O). Anal. calcd. For $C_{12}H_{11}FN_4O$, C, 58.53; H, 4.50; N, 22.75. Found: C, 58.69; H, 4.51; N, 22.80.

3-Hydroxy-*N*′-((1-methyl-1*H*-imidazol-2-yl)methylene) benzohydrazide (1 e): Yield: 74 %. M.P. 195–198 °C. ^{1}H-NMR (400 MHz, DMSO-d_6): δ = 3.96 (3H, s, CH_3), 6.98–7.04 (2H, m, imidazole CH), 7.28–7.33 (4H, m, 1,3-disubstituebenzen), 8.40 (1H, s, CH=N), 9.78 (1H, s, OH), 11.78 (1H, s, NH). ^{13}C-NMR (100 MHz, DMSO-d_6): δ = 35.53 (CH_3), 114.98, 118.58, 119.30, 126.04, 129.56, 130.12, 135.16, 140.59, 141.73, 157.97, 163.56 (C=O). Anal. calcd. For $C_{12}H_{12}N_4O_2$, C, 59.01; H, 4.95; N, 22.94. Found: C, 59.11; H, 4.94; N, 22.86.

4-Methyl-*N*′-((1-methyl-1*H*-imidazol-2-yl)methylene) benzohydrazide (1 f): Yield: 70 %. M.P. 188–190 °C. ^{1}H-NMR (400 MHz, DMSO-d_6): δ = 2.76 (3H, s, CH_3), 4.27 (3H, s, CH_3), 7.71–7.81 (4H, m, 1,4-disubstituebenzen, imidazole CH), 8.12 (1H, s, CH=N), 8.20 (2H, d, J = 6.80 Hz, 1,4-disubstituebenzen), 15.05 (1H, s, NH). ^{13}C-NMR (100 MHz, DMSO-d_6): δ = 21.56 (CH_3), 33.61 (CH_3), 124.08, 127.70, 128.10, 128.41, 128.69, 130.11, 130.76, 141.45, 163.31 (C=O). Anal. calcd. For $C_{13}H_{14}N_4O$, C, 64.45; H, 5.82; N, 23.13. Found: C, 64.24; H, 5.83; N, 23.17.

3-Bromo-*N*′-((1-methyl-1*H*-imidazol-2-yl)methylene) benzohydrazide (1 g): Yield: 69 %. M.P. 189–191 °C. ^{1}H-NMR (400 MHz, DMSO-d_6): δ = 3.96 (3H, s, CH_3), 7.05 (1H, s, imidazole CH), 7.36 (1H, s, imidazole CH), 7.49-7.53 (1H, m, 1,3-disubstituebenzen), 7.80 (1H, d, *J* = 8.00 Hz, 1,3-disubstituebenzen), 7.90 (1H, d, *J* = 7.76 Hz, 1,3-disubstituebenzen), 8.08 (1H, s, 1,3-disubstituebenzen), 8.40 (1H, s, CH=N). ^{13}C-NMR (100 MHz, DMSO-d_6): δ = 35.54 (CH_3), 122.31, 126.22, 127.35, 128.72, 129.72, 130.63, 131.36, 135.10, 136.01, 141.24, 162.01 (C=O). Anal. calcd. For $C_{12}H_{11}BrN_4O$, C, 46.93; H, 3.61; N, 18.24. Found: C, 47.05; H, 3.60; N, 18.20.

4-Nitro-*N*′-((1-methyl-1*H*-imidazol-2-yl)methylene) benzohydrazide (1 h): Yield: 66 %. M.P. 168–170 °C. ^{1}H-NMR (400 MHz, DMSO-d_6): δ = 3.98 (3H, s, CH_3), 7.07 (1H, s, imidazole CH), 7.38 (1H, s, imidazole CH), 8.14 (2H, d, *J* = 8.00 Hz, 1,4-disubstituebenzen), 8.38–8.42 (3H, d, *J* = 8.00 Hz, 1,4-disubstituebenzen, CH=N), 12.12 (1H, s, NH). ^{13}C-NMR (100 MHz, DMSO-d_6): δ = 35.54 (CH_3), 124.21, 126.33, 129.62, 129.76, 130.79, 139.35, 141.68, 149.77, 161.86 (C=O). Anal. calcd. For $C_{12}H_{11}N_5O_3$, C, 40.81; H, 3.14; N, 19.83. Found: C, 40.90; H, 3.15; N, 19.90.

3-Methoxy-*N*′-((1-methyl-1*H*-imidazol-2-yl)methylene) benzohydrazide (1 i): Yield: 73 %. M.P. 263–267 °C. ^{1}H-NMR (400 MHz, DMSO-d_6): δ = 3.83 (3H, s, CH_3), 3.97 (3H, s, OCH_3), 7.05 (1H, s, 1,3-disubstituebenzen), 7.16 (1H, d, *J* = 7.12 Hz, imidazole CH), 7.34 (1H, s, imidazole CH), 7.43-7.49 (3H, m, 1,3-disubstituebenzen), 8.42 (1H, s, CH=N), 11.82 (1H, s, NH). ^{13}C-NMR (100 MHz, DMSO-d_6): δ = 35.48(CH_3), 55.81 (3H, s, OCH_3), 113.34, 117.96, 120.22, 126.06, 129.57, 130.22, 135.10, 140.71, 141.61, 159.68, 163.22 (C=O). Anal. calcd. For $C_{13}H_{14}N_4O_2$, C, 60.45; H, 5.46; N, 21.69. Found: C, 60.51; H, 5.47; N, 21.74.

Crystallographic Studies

The single crystal X-ray diffraction measurements were carried out at 273.15 K on a Bruker D8 QUEST diffractometer with a rotation anode using graphite monochromated Mo Kα radiation at λ = 0.71073 Å. The data reduction was achieved with the Bruker SMART program.[26] The solution of crystal structure was performed by using Olex2 software.[27] Both structures were solved by Least Squares using the program SHEXL.[28] All-non-hydrogen atoms were refined anisotropically and hydrogen atoms were added at calculated positions. The molecular structure and geometrical parameters of the compounds were acquired by using MERCURY program.[29] Crystallographic data has been deposited with the Cambridge Crystallographic Data Center with CCDC No. 2246383 for compound **1 a** and 2246382 for compound **1 f**.

Anticancer Activity

The anticancer activities of the compounds **1 a**–**1 i** were determined by the absorbance values obtained from MTT assays. The MTT method was performed as previously described.[30] The anticancer activities of the compounds were evaluated against two cancer cell lines (C6 and HT-29). L929 healthy mouse fibroblast cells were used to evaluate the selectivity of the compounds. In this section, cisplatin was used as a reference drug in cell lines.

Carbonic Anhyrase I/II Inhibition Assay

Both of the hCA I and II isoforms we used in our study are enzymes that we previously purified, characterized, and stocked using the Sepharose-4B-L-Tyrosine-sulfanilamide affinity chromatography method.[31–34] The effect of these newly synthesized molecules on the activity of these enzymes was investigated using the esterase method. The Verpoorte test was used to assess the activity of both isoforms spectrophotometrically.[35–37] The amount of CA that converts *p*-nitrophenolate from its precursor, *p*-nitrophenylacetate, in three minutes at 348 nm (25 °C), is referred to as one CA unit.[37] The obtained data were used to compute new hydrazone derivative concentrations (IC_{50}), at which 50 % of the activities of hCA I and hCA II isoenzymes were inhibited. Acetazolamide (AAZ) was used as the standard drug in the study.[38]

Supporting Information

In the supporting information the researcher can view the full characterization data of compounds.

Author Contributions

HU and UAC conceived and designed the study, HU performed the synthesized compounds and Crystallographic Studies, UA performed the analysed compounds. HEB performed the anticancer activity, OK and UMK performed the Carbonic Anhyrase I/II Inhibition Assay. All authors reviewed and edited the manuscript. All authors read and approved the manuscript.

Acknowledgements

The authors acknowledge to Scientific and Technological Research Application and Research Center, Sinop University, Turkey, for the use of the Bruker D8 QUEST diffractometer."

Conflict of Interests

The authors declare no conflict of interest.

Data Availability Statement

The data that support the findings of this study are available in the supplementary material of this article.

Keywords: Anticancer · hCA I/II · Hydrazone · Imidazole · X-ray

[1] U. Acar Çevik, I. Celik, A. Işık, I. Ahmad, H. Patel, Y. Özkay, Z. A. Kaplancıklı, *J. Biomol. Struct. Dyn.* **2022**, 1–15.
[2] K. Kucukoglu, N. Faydali, D. Bul, H. Nadaroglu, B. Sever, M. D. Altıntop, B. Ozturk, I. Guzel, *J. Mol. Struct.* **2023**, *1276*, 134699.
[3] D. Moi, S. Vittorio, A. Angeli, G. Balboni, C. T. Supuran, V. Onnis, *Molecules.* **2023**, *28*(1), 91.
[4] B. D. Vanjare, N. G. Choi, Y. S. Eom, H. Raza, M. Hassan, K. H. Lee, S. J. Kim, *Mol. Diversity* **2023**, *27*(1), 193–208.
[5] M. F. Said, R. F. George, A. Petreni, C. T. Supuran, N. M. Mohamed, *J. Enzyme Inhib. Med. Chem.* **2022**, *37*(1), 701–717.
[6] F. Liguori, S. Carradori, R. Ronca, S. Rezzola, S. Filiberti, F. Carta, M. Turati, C. T. Supuran, *J. Enzyme Inhib. Med. Chem.* **2022**, *37*(1), 1857–1869.
[7] S. A. Güngör, M. Köse, M. Tümer, C. Türkeş, Ş. Beydemir, *J. Biomol. Struct. Dyn.* **2022**, 1–11.
[8] A. Ahmed, M. Aziz, S. A. Ejaz, P. A. Channar, A. Saeed, S. Zargar, T. A. Wani, A. Hamad, Q. Abbas, H. Raza, S. J. Kim, *Biomol. Eng.* **2022**, *12*(11), 1696.
[9] M. Tapera, H. Kekeçmuhammed, B. Tüzün, E. Sarıpınar, Ü. M. Koçyiğit, E. Yıldırım, M. Doğan, Y. Zorlu, *J. Mol. Struct.* **2022**, *1269*, 133816.
[10] M. T. Muhammed, E. R. Mustafa, S. Akkoc, *J. Mol. Struct.* **2023**, *1282*, 135066.
[11] H. Aziz, A. Saeed, F. Jabeen, M. A. Khan, A. U. Rehman, M. Q. Khan, M. Saleem, *J. Mol. Struct.* **2023**, 134924.
[12] S. Slassi, M. Aarjane, A. Amine, *J. Mol. Struct.* **2022**, *1255*, 132457.
[13] R. Chen, R. Francese, N. Wang, F. Li, X. Sun, B. Xu, J. Liu, Z. Liu, M. Donalisio, D. Lembo, G. C. Zhou, *Eur. J. Med. Chem.* **2023**, 115081.
[14] S. Poyraz, H. A. Döndaş, J. M. Sansano, S. Belveren, C. Yamali, M. Ülger, N. Y. Döndaş, B. N. Saglık, C. M. Pask, *J. Mol. Struct.* **2023**, *1273*, 134303.
[15] M. El-Shahat, W. I. El-Sofany, A. G. A. Soliman, M. Hasanin, *J. Mol. Struct.* **2022**, *1250*, 131727.
[16] Ö. Aslanhan, E. Kalay, F. S. Tokalı, Z. Can, E. Şahin, *J. Mol. Struct.* **2023**, 135037.
[17] F. Yang, J. Zhao, G. Chen, H. Han, S. Hu, N. Wang, J. Wang, Y. Chen, Z. Zhou, B. Dai, Y. Hou, Y. Liu, *Bioorg. Chem.* **2023**, *133*, 106432.
[18] M. İ. Han, N. İmamoğlu, *ACS Omega.* **2023**.
[19] M. Fan, W. Yang, L. Liu, Z. Peng, Y. He, G. Wang, *Bioorg. Chem.* **2023**, 106384.
[20] M. S. Lone, M. M. Mubarak, S. A. Nabi, F. R. Wani, S. Amin, S. Nabi, H. A. Kantroo, M. Samim, S. Shafi, S. Ahmad, Z. Ahmad, S. O. Rizvi, K. Javed, *Med. Chem. Res.* **2023**, 1–19.
[21] Q. Wang, X. Tu, X. Wang, Q. Cai, L. Yu, X. Zhang, J. Yi, Y. Wu, G. Xie, H. Yuan, M. Li, X. Zhang, Z. Zeng, Y. Su, *Bioorg. Chem.* **2022**, *128*, 106069.
[22] U. Acar Cevik, B. Nurpelin Saglik, Y. Ozkay, Z. Canturk, J. Bueno, F. Demirci, A. Savas Koparal, *Curr. Pharma. Des.* **2017**, *23*(15), 2276–2286.
[23] A. M. Rozada, F. A. Rodrigues-Vendramini, D. S. Goncalves, F. A. Rosa, E. A. Basso, F. A. Seixas, E. S. Kioshima, G. F. Gauze, *Bioorg. Med. Chem. Lett.* **2020**, *30*(14), 127244.
[24] B. B. Gao, A. Clermont, S. Rook, S. J. Fonda, V. J. Srinivasan, M. Wojtkowski, J. G. Fujimoto, R. L. Avery, P. G. Arrigg, S. E. Bursell, L. P. Aiello, E. P. Feener, *Nat. Med.* **2007**, *13*(2), 181–188.
[25] C. T. Supuran, *Curr. Pharm. Des.* **2008**, *14*(7), 603–614.
[26] SMART, Bruker AXS, 2000.
[27] O. V. Dolomanov, L. J. Bourhis, R. J. Gildea, J. A. K. Howard, H. Puschmann, *J. Appl. Crystallogr.* **2009**, *42*, 339–341.
[28] G. M. Sheldrick, *Acta Crystallogr.* **2015**, A71.
[29] C. F. Macrae, P. R. Edgington, P. McCabe, E. Pidcock, G. P. Shields, R. Taylor, M. Towler, *J. Appl. Crystallogr.* **2006**, *39*, 453–457.
[30] A. Isık, U. A. Çevik, I. Çelik, H. E. Bostancı, A. Karayel, G. Gündoğdu, U. Ince, A. Koçak, Y. Ozkay, Z. A. Kaplancıklı, *J. Mol. Struct.* **2022**, *1270*, 133946.
[31] H. Gezegen, M. B. Gürdere, A. Dinçer, O. Özbek, Ü. M. Koçyiğit, P. Taslimi, M. Ceylan, *Arch. Pharm.* **2021**, *354*(4), 2000334.
[32] J. A. Verpoorte, S. Mehta, J. T. Edsall, *J. Biol. Chem.* **1967**, *242*(18), 4221–4229.
[33] D. D. Armstrong, Subchapter S-lts Opportunities and Pitfalls. New York Certified Public Accountant (pre-1986), **1996**, *36*(000008), 573.
[34] U. M. Kocyigit, A. Ş. Taşkıran, P. Taslimi, A. Yokuş, Y. Temel, İ. Gulçin, *J. Biochem. Mol. Toxicol.* **2017**, *31*(11), e21972.
[35] Ü. M. Koçyiğit, M. Doğan, H. Muğlu, P. Taslimi, B. Tüzün, H. Yakan, H. Bal, E. Güzel, İ. Gülçin, *J. Mol. Struct.* **2022**, *1264*, 133249.
[36] M. Doğan, Ü. M. Koçyiğit, M. B. Gürdere, M. Ceylan, Y. Budak, *Med. Oncol.* **2022**, *39*(10), 157.
[37] Ü. M. Koçyiğit, P. Taslimi, B. Tüzün, H. Yakan, H. Muğlu, E. Güzel, *J. Biomol. Struct. Dyn.* **2022**, *40*(10), 4429–4439.
[38] E. Güzel, Ü. M. Koçyiğit, P. Taslimi, İ. Gülçin, S. Erkan, M. Nebioğlu, B. S. Arslan, İ. Şişman, *J. Biomol. Struct. Dyn.* **2022**, *40*(2), 733–741.

Manuscript received: April 25, 2023